Biotechnol. Bioprocess Eng. **1999**, 4, 51-58

Mathematical Model for a Three-Phase Fluidized Bed Biofilm Reactor in Wastewater Treatment

Jeong-Woo Choi[1]*, Juhong Min[1], Won-Hong Lee[1], and Sang Back Lee[2]

[1]Department of Chemical Engineering, Sogang University, Seoul 121-742, Korea
[2]Department of Chemical Engineering, Cheju National University, Cheju 690-756, Korea

A mathematical model for a three phase fluidized bed bioreactor (TFBBR) was proposed to describe oxygen utilization rate, biomass concentration and the removal efficiency of Chemical Oxygen Demand (COD) in wastewater treatment. The model consisted of the biofilm model to describe the oxygen uptake rate and the hydraulic model to describe flow characteristics to cause the oxygen distribution in the reactor. The biofilm model represented the oxygen uptake rate by individual bioparticle and the hydrodynamics of fluids presented an axial dispersion flow with back mixing in the liquid phase and a plug flow in the gas phase. The difference of settling velocity along the column height due to the distributions of size and number of bioparticle was considered. The proposed model was able to predict the biomass concentration and the dissolved oxygen concentration along the column height. The removal efficiency of COD was calculated based on the oxygen consumption amounts that were obtained from the dissolved oxygen concentration. The predicted oxygen concentration by the proposed model agreed reasonably well with experimental measurement in a TFBBR. The effects of various operating parameters on the oxygen concentration were simulated based on the proposed model. The media size and media density affected the performance of a TFBBR. The dissolved oxygen concentration was significantly affected by the superficial liquid velocity but the removal efficiency of COD was significantly affected by the superficial gas velocity.

Key words: three phase fluidized bed biofilm reactor, wastewater treatment, mathematical model, oxygen concentration, COD

INTRODUCTION

In both wastewater treatment and fermentation process, a fluidized bed biofilm reactor (FBBR) has been demonstrated to outperform other reactor configurations such as the activated sludge system and packed bed bioreactor [1,2]. The wastewater flows upward through a bed at the sufficient velocity to fluidize the biofilm covered media in a FBBR. This bioreactor has many advantages such as large available surface area for the cell growth per unit volume of the reactor, relatively small head loss, no clogging, and easiness of carrier removal. [3-5].

However, it has been known that carbonaceous and nitrogenous oxidation in preoxigenated two-phase fluidized bed biofilm reactor is limited by oxygen transfer in wastewater treatment. This phenomenon leads to decrease of the height of an efficient column (HEC) due to the oxygen depletion in upper part of a fluidized bed [3]. A three phase fluidized bed bioreactor (TFBBR) has been used to overcome this disadvantage [1,2]. Since a TFBBR allows continuous treatment with the relatively low pressure drop and the high removal efficiency of Chemical Oxygen Demand (COD), a TFBBR has been applied in the biological wastewater treatment processes.

To provide a rational criteria for design and operation of a TFBBR in wastewater treatment, a mathematical model to describe the oxygen utilization in a TFBBR should be developed since the model can identify important system variables and serve a basis for system optimization. However mathematical model to describe the oxygen utilization for a TFBBR in wastewater treatment has not been well developed [1-7]. Especially oxygen concentration profile along the bed height is very important biomass concentration, COD removal efficiency and HEC can be presented. Since the principal advantage of a TFBBR is the reduction in reactor size caused by the high biomass concentration, an understanding of the factors that affect the biomass concentration is important to analyze a TFBBR [8]. Thus the mathematical model to describe the oxygen concentration and biomass concentration should be developed to evaluate the performance of a TFBBR.

In this paper, the mathematical model for a TFBBR in wastewater treatment process is proposed to describe the oxygen concentration distribution. The model consists of the biofilm model that describes the oxygen uptake rate and the hydraulic model that presents characteristics of liquid and gas phase. The proposed model is able to predict the biomass concentration and oxygen concentration profile along the bed height. The validation of the model is done in comparison with the experimental data and various parameters affecting the performance of a TFBBR are estimated using the model. The removal efficiency of COD is also evaluated based on biomass concentration and dissolved oxygen concentration profile by the simulation.

* Corresponding author
Tel: +82-2-705-8480 Fax: +82-2-711-0439
e-mail : jwchoi@ccs.sogang.ac.kr

MODEL

A TFBBR is considered to be operated at the steady state condition, in which spherical media of uniform size is covered with biofilm of different thickness. The mathematical model for a TFBBR includes the following elements like a conventional two phase FBBR [9]; (1) a biofilm model to represent the oxygen uptake rate by individual bioparticles, (2) a hydraulic model to represent the flow characteristics in the bed, (3) an overall bioreactor model to consist of the biofilm model and hydraulic models to yield oxygen concentration and biomass concentration as a function of the axial position in a TFBBR.

The biomass concentration and the degree of bed expansion are calculated using the hydraulic model at given operating conditions and design parameters. Simultaneously the information generated from the hydraulic model is applied to the biofilm model to calculate oxygen uptake rates. An effectiveness factor that expresses mass transfer resistance is calculated in the biofilm model.

Biofilm Model

Oxygen transfer and uptake in the TFBBR can be described by the following steps [10]; (1) transport of oxygen from the bulk gas to the bubble interface, (2) transport of oxygen from the bubble interface to the bulk liquid phase, (3) transport of oxygen from the bulk liquid phase to the biofilm interface, (4) transport of oxygen within the biofilm, (5) oxygen uptake within the biofilm.

Mass transfer resistance in gas phase, step (1), is negligible compared to those in other steps [10]. External mass transfer resistance in liquid phase, step (3), is a function of Reynolds number of liquid flow. Reynolds number is large enough to neglect the resistance in step (3) because relative velocity is high to fluidize the bioparticle. The experimental results showed that the negligence of the external mass transfer resistance in step (3) can be reasonably negligible [7]. The diffusion of oxygen within the biofilm lead that the oxygen partially penetrates into the biofilm. Step (4) and Step (5) take place simultaneously and be modeled from the characteristics of the biofilm. In step (5), the oxygen uptake rate can be described by the Monod kinetics.

$$r_{O_2} = \frac{\mu_m C}{Y_{O_2}(k_{O_2}+C)}\rho_{bd} \tag{1}$$

where mm is maximum specific growth rate; k_{O_2} is saturation constant of oxygen; ρ_{bd} is the biofilm dry density; C is the oxygen concentration; Y_{O_2} is a yield of biomass upon oxygen. Since the oxygen concentration in the biofilm is greater than 1 ppm and the values of k_{O_2} are 0.032~0.53 ppm [10], the reaction rate follows the intrinsic zero order kinetics.

$$r_{O_2} = \frac{\mu_m}{Y_{O_2}}\rho_{bd} = \kappa_o \rho_{bd} \tag{2}$$

where κ_o is the intrinsic zero-order rate constant.

The biofilm kinetics for oxygen utilization is derived based on the model proposed by Shieh [11]. The Shieh's model can be applied to oxygen utilization though its model is proposed for the nutrient utilization. The physical system and the associated notations are depicted in Fig. 1. At steady state condition the continuity equation of oxygen in the biofilm is

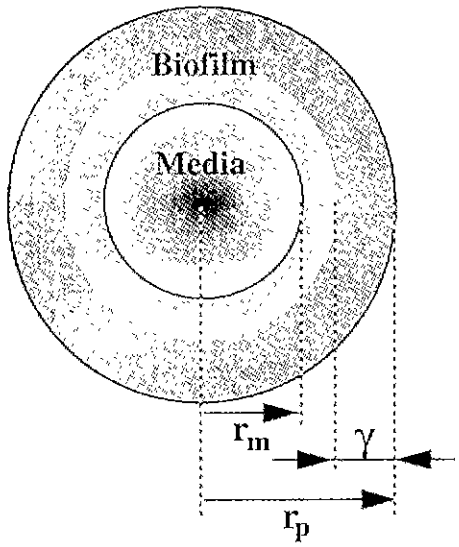

Fig. 1. Schematic diagram of bioparticle, r_p, radius of bioparticle; r_m, radius of media; γ, radial distance at which the oxygen concentration ceases.

$$\frac{D_{ec}}{r^2}\frac{d}{dr}\left(r^2\frac{dC}{dr}\right) = r_{O_2} = \rho_{bd}\kappa_o \tag{3}$$

The associated boundary conditions are

$$C = C_l \qquad \text{at } r = r_p \tag{4}$$

$$\frac{dC}{dr} = 0, \quad C = 0, \quad \text{at } r = r_p - \gamma, \quad (0 \le \gamma \le r_p - r_m) \tag{5}$$

where D_{ec} is the effective diffusivity of oxygen in the biofilm and C_l is the dissolved oxygen concentration. The penetration depth, γ, is used to present that oxygen penetrates partially into the biofilm, which is due to internal mass transfer resistance. The following equation is obtained by integration of Eq. 3 with boundary conditions, Eqs. 4 and 5 [11].

$$1-\left(\frac{r_p-\gamma}{r_p}\right)^3 = 3.012(\rho_{bd}\kappa_o/D_{ec})^{-0.45} r_p^{-0.9} C_l^{0.45} \tag{6}$$

For intrinsic zero order reaction, effectiveness factor can be presented as the ratio of biofilm volume which substrate can penetrate to total biofilm volume. Thus effectiveness factor η_o is, therefore, presented as the following equation [11,12].

$$\eta_o = \frac{1-\left(\frac{r_p-\gamma}{r_p}\right)^3}{1-\left(\frac{r_m}{r_p}\right)^3} = \frac{3.012(\rho_{bd}\kappa_o/D_{ec})^{-0.45} r_p^{-0.9}}{1-\left(\frac{r_m}{r_p}\right)^3} C_l^{0.45} \tag{7}$$

Thus the oxygen uptake rate per unit volume of the reactor, R_V, is presented as

$$R_V = \eta_o \kappa_o \chi \tag{8}$$

Herein, biomass concentration, χ can be expressed as

$$\chi = \rho_{bd}(1-\varepsilon_{lg})\left(1-\left(\frac{r_m}{r_p}\right)^3\right) \quad (9)$$

where ε_{lg} is the bed porosity. In order to calculate biomass concentration, the bed porosity should be obtained. Bed porosity in a TFBBR is a function of gas and liquid velocities and other physical parameters at given operating conditions. To express the bed porosity, various experimental and theoretical correlations for bed porosity have been reported [2,13]. Since these correlations presented for bed porosity without biofilm in the fluidized bed reactor, it is different from that of a TFBBR. In a TFBBR the changes of particle density and size due to the biofilm growth causes the change of settling velocity of bioparticles and bed height of the reactor. Thus the change of settling velocity due to the biofilm growth should included in the correlation for bed porosity of a TFBBR.

The correlation developed by Dakshinamurty *et al.* [14] is used to express the bed porosity of a TFBBR.

$$\varepsilon_{lg} = 2.12\left(\frac{U_l}{U_t}\right)^{0.41}\left(\frac{\mu_l U_g}{\sigma}\right)^{0.08} \quad N_{Re}<500 \quad (10)$$

where U_l, U_g and U_t are superficial liquid velocity, superficial gas velocity and terminal velocity of liquid, respectively, and μ_l is liquid viscosity and σ is surface tension of liquid. Terminal velocity can be expressed with drag coefficient, C_D.

$$U_t = \left[\frac{4(\rho_p-\rho_l)gD_p}{3C_D\rho_p}\right]^{1/2} \quad (11)$$

where ρ_p and ρ_l are density of bioparticle and liquid, respectively. D_p is the bioparticle diameter. Since the range of Reynolds number, N_{Re}, in a TFBBR is expressed with the Stoke's law, the correlation of drag coefficient for the spherical bioparticle is as follows [7].

$$C_D = 36.66N_{Re}^{-0.67} \quad (12)$$

Bioparticle density can be calculated with the following equation.

$$\rho_p = \rho_m\left(\frac{r_m}{r_p}\right)^3 + \rho_{bw}\left[1-\left(\frac{r_m}{r_p}\right)^3\right] \quad (13)$$

where ρ_m and ρ_{bw} are densities of media and wet biofilm, respectively. Thus biomass concentration in Eq. 9 can be calculated by combination of Eqs. 10-13. Biomass concentration is a function of the characteristic parameters of a TFBBR such as the superficial velocity of gas and liquid, density of biofilm, and media size. By controlling the superficial velocity of gas and liquid, density of biofilm and media size, the desired biomass concentration can be obtained.

Hydraulic Model

A conventional reactor hydraulic model of a three phase fluidized bed (TFB) has been developed with several assumptions [15-17]. In the development of a TFBBR model, the following assumptions are used to simplify the model; (1) no gradient of radial direction in the gas and liquid phase, (2) no oxygenation reaction in the liquid phase, (3) pseudo steady state condition, (4) no wake formation in the fluid phase. According to the above assumptions, the mass balances for oxygen can be formulated as follows.

For the liquid phase,

$$\frac{d}{dz}\left(E_{zl}\varepsilon_l\frac{dC_l}{dz}\right)-U_l\frac{dC_l}{dz}+k_l\bar{a}_g\left(\frac{C_g}{M}-C_l\right)-k_sa_s(C_l-C_s)=0 \quad (14)$$

The associated boundary conditions are

$$C_l = C_h + E_{zl}\frac{dC}{dz} \qquad \text{at } z=0$$

$$\frac{dC}{dz} = 0 \qquad \text{at } z=H$$

where z is axial position; E_{zl} is axial dispersion coefficient; ε_l is liquid porosity, k_l is mass transfer coefficient between gas and liquid phase; $\bar{a}_g$ is average interfacial area of gas bubble per unit volume of reactor; M is Henry constant; k_s mass transfer coefficient between liquid and solid phase; a_s is average interfacial area of solid per unit volume of reactor. C_g, C_s and C_h are concentration of gas phase, solid phase and liquid phase at inlet position, respectively.

For the solid phase,

$$k_sa_s(c_l-C_s)-R_v=0 \quad (15)$$

For the gas phase,

$$U_g\frac{dC_g}{dz}+k_l\bar{a}_g\left(\frac{C_g}{M}-C_l\right)=0 \quad (16)$$

The associated boundary condition is

$$C_g = C_{gi} \qquad \text{at } z=0$$

where C_{gi} are concentration of gas phase at inlet position.

Combining Eqs. 14 and 15 gives

$$\frac{d}{dz}\left(E_{zl}\varepsilon_l\frac{dC_l}{dz}\right)-U_l\frac{dC_l}{dz}+k_l\bar{a}_g\left(\frac{C_g}{M}-C_l\right)-R_V=0 \quad (17)$$

Oxygen uptake rate per reactor volume, R_V, is derived by Eqs. 7-9.

$$R_V = \eta_o\kappa_o\chi = 3.012(\rho_{bd}\kappa_o)^{0.55}D_{ec}^{0.45}r_p^{-0.9}C_l^{0.45}(1-\varepsilon_{lg}) = \Phi\varepsilon_sC_l^{0.45} \quad (18)$$

where $\Phi = 3.012(\rho_{bd}\kappa_o)^{0.55}D_{ec}^{0.45}r_p^{-0.9}$ and $\varepsilon_s = (1-\varepsilon_{lg})$.

Eq. 18 is substituted into Eq. 17.

$$\frac{d}{dz}\left(E_{zl}\varepsilon_l\frac{dC_l}{dz}\right)-U_l\frac{dC_l}{dz}+k_l\bar{a}_g\left(\frac{C_g}{M}-C_l\right)-\Phi\varepsilon_sC_l^{0.45}=0 \quad (19)$$

In dimensionless form, Eqs. 17-19 are reduced to

$$\frac{d}{d\theta}\left(\frac{1}{Pe}\frac{d\bar{C}}{d\theta}\right)-\frac{d\bar{C}}{d\theta}+\beta(\delta\bar{G}-C)-\omega\bar{C}^{0.45}=0 \quad (20)$$

$$\frac{d\bar{G}}{d\theta} + \lambda(\delta\bar{G} - \bar{C}) = 0 \quad (21)$$

where $\bar{C} = \frac{C}{C_i}$, $\beta = \left(\frac{k_l \bar{a}_g H}{U_l \varepsilon_l}\right)$, $\lambda = \frac{k_l \bar{a}_g H C_{li}}{U_g \varepsilon_g C_{gi}}$,

$\theta = \frac{z}{H}$, $\delta = \left(\frac{C_{gi}}{C_{li} M}\right)$, $\omega = \frac{\Phi \varepsilon_s C_l^{0.45}}{\varepsilon_l U_l}$,

and Peclet number is defined as $Pe = \frac{U_l D_p}{E_{zl}}$

The boundary conditions become [16,18]

$$1 = \bar{C} - \frac{1}{Pe}\frac{d\bar{C}}{d\theta} \quad \text{at} \quad \theta = 0$$
$$1 = \bar{G} \quad (22)$$

$$\frac{d\bar{C}}{d\theta} = 0 \quad \text{at} \quad \theta = 1 \quad (23)$$

In Eqs. 20 and 22, the axial dispersion coefficient is changed along the bed height because particle size distribution occurs along the bed height due to the biofilm growth that causes the change of particle density. The axial dispersion coefficient is correlated with Pe number. El-Temtany [20] reported the modified Pe number that accounts the change of axial dispersion coefficient in two phase fluidized bed. In a TFBBR, Pe number reported by El-Temtany [20] should be modified to represent the presence of the distribution of biofilm mass along the bed height. The modified Pe number should include the thickness of biofilm and density of bioparticle in order to account of the phenomenon in which large bioparticles exist in the upper zone in a TFBBR, which is different from that of a fluidized bed without biofilm. The modified Pe that accounts the thickness of biofilm and density of bioparticle is proposed as

$$Pe = aN_{Re,p}^{1.156} D_T^{-1.156} \left(\frac{\rho_s - \rho_L}{\rho_L}\right)^b \left(\frac{D_p}{D_m}\right)^c \quad (24)$$

where a, b, c are unknown parameters; $N_{Re,p}$ is Reynolds number related with particle; D_T is the bed diameter; ρ_s is the density of particle; ρ_L is the density of liquid; D_m is the diameter of media.

RESULTS AND DISCUSSION

Validation of Model

All parameters were known from the experiments [3, 20,21] except a, b and c. The experimental data [3], C_l vs. height, is compared to the model predictions by choosing parameter a, b and c that give best fit of the model to the data in a TFBBR. A nonlinear parameter estimation package, Nonlinear Parameter Estimation Package (NONLIN), is used [22] and this employs a weighting factor for the residuals proportional $\bar{C}$ so that the information near the end of bed height is highlighted while Eqs. 8-13 and Eqs. 18-24 were solved simultaneously with finite difference method [23].

In a TFBBR experiment to remove organic carbon in wastewater treatment were performed and oxygen concentration profile along the bed height was obtained as shown in Fig. 2 [3]. The model results with

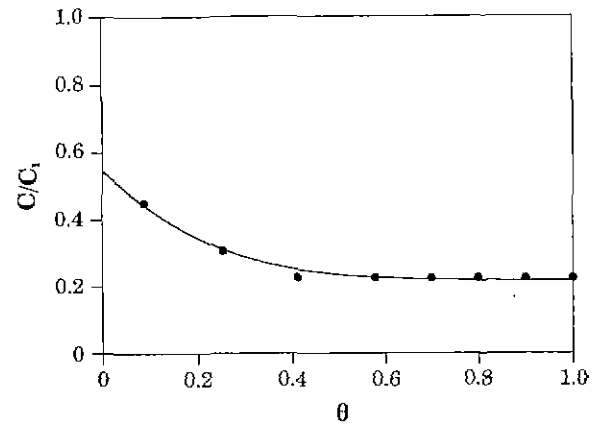

Fig. 2. Experimental and theoretical results for the dissolved oxygen concentration in a TFBBR.

Table 1. Experimental values in simulation (All values except D_{ec} and K_o are in reference [3], D_{ec} and k_o are in reference [20] and [21], respectively

C_{gi}	2.795×10^{10}	U_g	1.06
C_{li}	1.397×10	U_l	0.5036
D	1.5×10^{-5}	ρ_{bd}	0.03
D_T	9.4	ρ_l	1.0
H	75	ρ_m	1.7
$k_l \bar{a}$	1.87×10	K_o	1.62×10^{-5}
r_m	0 043	μ_l	0.9×10^{-2}

the estimates are shown as the smooth, and solid curves in Fig. 2. It can be seen that the model is quite consistent over the whole bed height and is able to approximate all experimental data fairly well. The experimental data shown were used for parameter estimation in subroutines of a program. The estimated values of parameters, a, b and c, are 0.0625, 0.5 and -1.14, respectively.

Fig. 2 shows that constant oxygen concentration is observed as constant in the upper part of bed and oxygen concentration gradually decreases in the low part of bed. The reason for this result may be that oxygen uptake rate in bioparticle and oxygen transfer rate from gas phase decrease, and axial dispersion coefficient in liquid phase increases due to the existence of distribution of size and number of bioparticle along bed height. The size- and number-distribution of bioparticle along the bed height are induced by biofilm growth. Bioparticles with thick biofilm are in upper zone of bed and those with thin biofilm are in lower part of bed because the density of bioparticle is reduced as biofilm grows. The increase of biofilm thickness along bed height makes the number of bioparticle to decrease, oxygen uptake rate per unit reactor volume to be reduced and axial dispersion coefficient to increase along bed height. Thus axial dispersion coefficient becomes larger at upper zone of bed compared with at lower zone of bed. The proposed mathematical model can predict the change of biomass concentration and oxygen concentration along bed height with the account of the size- and number-distribution of bioparticle in the bed.

Simulation to Investigate the Effect of Operating Parameters

The proposed model for a TFBBR can describe the

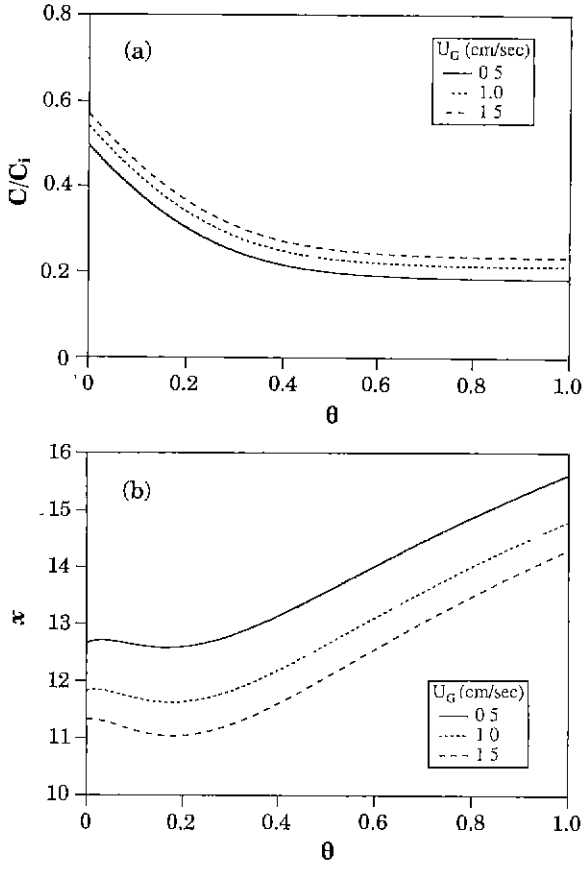

Fig. 3. Effect of sperficial gas velocity on (a) the dissolved oxygen concentration and (b) biomass concentration.

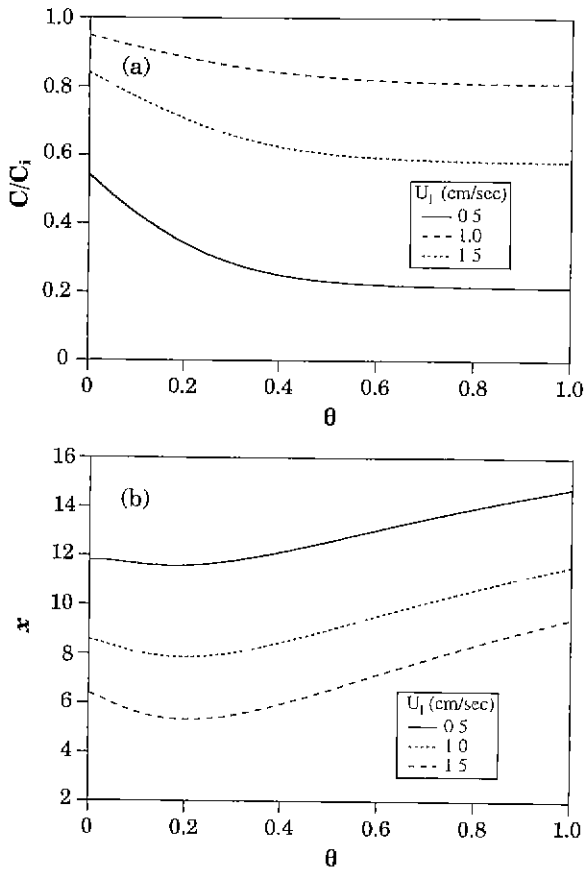

Fig. 4. Effect of sperficial liquid velocity on (a) the dissolved oxygen concentration and (b) biomass concentration.

hydrodynamic characteristics in addition to the oxygen utilization rate. The performance of a TFBBR can be evaluated using the proposed model for the oxygen uptake rate and biomass concentration which are directly related with eliminated COD amount of the organic removal in wastewater treatment. The performance of a TFBBR is influenced by operating parameters such as the relative superficial velocities of gas and liquid, media size and density that affect the bed porosity and expanded bed height. The effect of change of the operating parameters on dissolved oxygen concentration and biomass concentration are simulated using the model.

Fig. 3 shows that the change of the superficial gas velocity affects the dissolved oxygen concentration in liquid phase and biomass concentration. It is observed that oxygen transfer rate from the gas phase increased slightly as superficial gas velocity increases because mass transfer coefficient and the oxygen concentration in gas phase is strongly related to superficial gas velocity. Biomass concentration decreases slightly as superficial gas velocity increases since solid porosity is a function of superficial gas velocity and decreases slightly as superficial gas velocity increases.

The dissolved oxygen concentration and biomass concentration are more affected by superficial liquid velocity than that by superficial gas velocity as shown in Fig. 4. As superficial liquid velocity increases, the contact time to be required for microbes to use up dissolved oxygen in liquid phase decreases. Thus the increase of superficial liquid velocity causes the profile of dissolved oxygen concentration to be up. Biomass concentration is strongly affected by liquid superficial

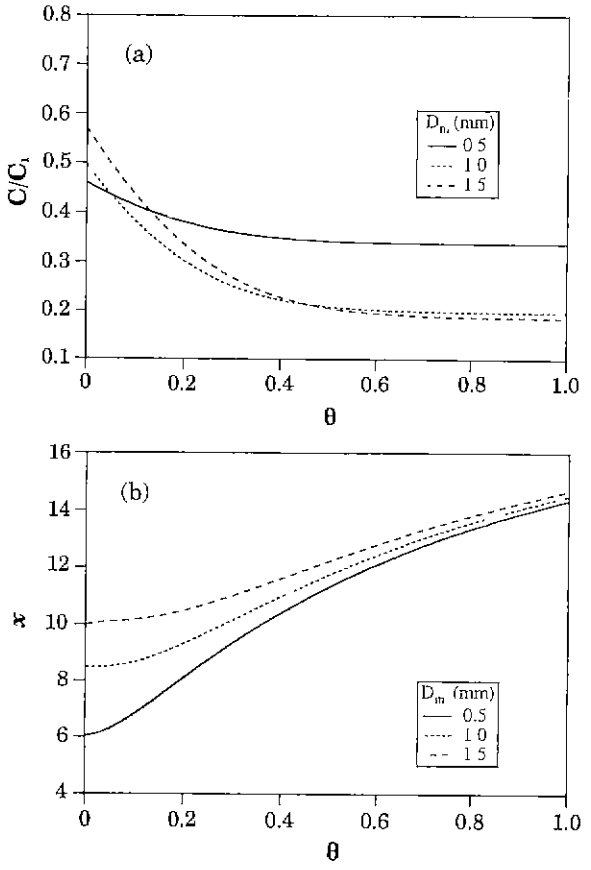

Fig. 5. Effect of media size on (a) the dissolved oxygen concentration and (b) biomass concentration.

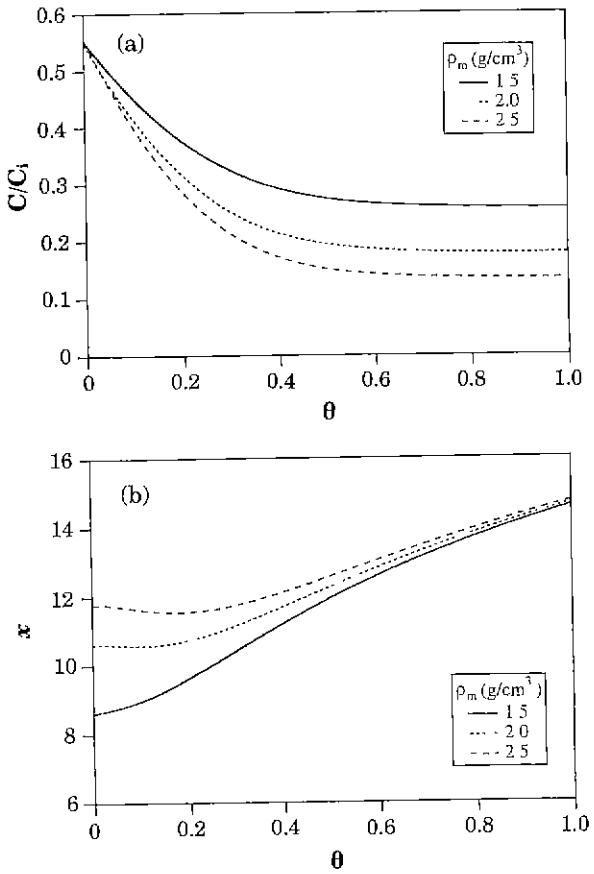

Fig. 6. Effect of media density on (a) the dissolved oxygen concentration and (b) biomass concentration.

velocity because solid porosity is more affected by superficial liquid velocity than by superficial gas velocity. Thus in the operation of TFBBR the superficial liquid velocity should be maintained at the minimum fluidization velocity at which the fluidization of solid particles occurs by upflow of liquid.

The effect of media size on the performance of a TFBBR is shown in Fig. 5. It is found that biomass concentration increases as media size increases, which causes the dissolved oxygen concentration to decreases. The settling velocity of bioparticle increases due to the increase of media size and thus most bioparticles exists in the lower zone of bed. In the lower zone of bed, biomass concentration significantly increases by the change of media size that cause the existence of the large number of bioparticle. However, in the upper zone, biomass concentration with larger media is not largely different from that with smaller media. Biomass concentration decreases as media size decreases, which results in the decrease of oxygen uptake by biomass and excessive bed expansion.

The impact of media density on the performance of a TFBBR is shown in Fig. 6. It presents that bed expansion is lessened by the increase of media density at given superficial liquid velocity and use of heavier media yields a higher biomass concentration in a TFBBR. The reason of this result is that the settling velocity of bioparticle with heavier media is higher than that with lighter media. Dissolved oxygen concentration decreases as media density increases since the amount of oxygen uptake per unit reactor volume increases due to the higher biomass concentration.

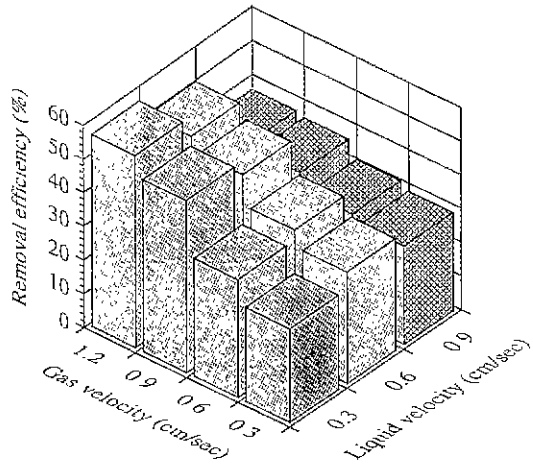

Fig. 7. Effects of superficial velocity of liquid and gas on the removal efficiency of a TFBBR.

The use of heavier media allows a TFBBR to have the high removal efficiency of COD. However, higher energy requirement and other operating problems occur for the fluidization of heavy media, so that the advantages with heavy media must be considered with several problems.

Removal Efficiency of COD

The removal efficiency of organic pollutants can be calculated with total oxygen mass consumed that is obtained from oxygen uptake rate and biomass concentration. The ratio of COD removal to oxygen consumption is expressed as [7].

$$\frac{\text{COD eliminated}}{\text{O}_2 \text{ consumed}} = 3.4$$

The effects of superficial velocities of liquid and gas on removal efficiency are represented at given operating condition as shown in Fig. 7. The removal efficiency is nearly constant or slightly decreases as superficial liquid velocity increases. The reason is that dissolved oxygen concentration increases as superficial velocity of liquid increases, which reduces biomass concentration and contact time between liquid and biofilm as shown in Fig. 5. Thus total oxygen consumption amount is nearly constant due to the counter effect between dissolved oxygen concentration and biomass concentration. At high superficial liquid velocity the dissolved oxygen concentration increases slightly, and biomass concentration and contact time decreases at the same degree, so that removal efficiency is low at all range of superficial gas velocity. The removal efficiency is strongly related to superficial gas velocity as shown in Fig. 7. The efficiency increases as superficial gas velocity increases. The reason is that mass transfer coefficient is a function of superficial gas velocity, so that more amount of oxygen from the gas phase is transferred to the liquid phase as superficial gas velocity increases. However the contact time between liquid and biofilm is nearly the same at any superficial gas velocity since the fluidization of bioparticle is mainly done by upflow of liquid.

NOMENCLATURE

a : Parameter in Eq. 1 [-]
$\bar{a}$: Average interfacial area per unit volume of reactor [cm^{-1}]
b : Parameter in Eq. 1 [-]
c : Parameter in Eq. 1 [-]
C : Oxygen concentration [g cm^3]
C_l : Oxygen concentration in the liquid phase [g cm^{-3}]
$\bar{C}$: Dimensionless oxygen concentration in the liquid phase [-]
C_D : Drag coefficient [-]
D : Diameter [cm]
D_{ec} : Effective diffusivity of oxygen in the biofilm [cm^2/sec]
E_{zl} : Axial dispersion coefficient [cm^2/sec]
$\bar{G}$: Dimensionless oxygen concentration in the gas phase [-]
H : Expanded bed height [cm]
k : Mass transfer coefficient [cm^2/sec]
M : Henry constant [-]
N_{Re} : Reynolds number, $\frac{U_l D_p \rho_l}{\mu_l}$ [-]
$N_{Re,p}$: Reynolds number of media, $\frac{U_l D_m \rho_l}{\mu_l}$ [-]
P_e : Peclet number, $\frac{U_l D_p}{E_{zl}}$ [-]
R_V : Observed oxygen conversion rate per unit TFBBR volume [g/cm^3sec]
r : Radial distance [cm]
r_{O2} : Oxygen consumption rate [g/cm^3sec]
U : Superficial phase velocity [cm/sec]
U_t : Terminal settling velocity of bioparticle [cm/sec]
Y_{O2} : Yield of biomass upon oxygen [-]

Greek symbols

β : $\frac{k_l \bar{a} H}{U_l \varepsilon_l}$ [-]
δ : $\frac{C_{gi}}{C_{li} M}$ [-]
γ : Radial distance at which the oxygen concentration ceases [cm]
ε : Porosity [-]
η_o : Effectiveness factor for intrinsic zero order reaction [-]
θ : Dimensionless length [-]
κ_o : Intrinsic zero order rate constant for oxygen [sec]
λ : $\frac{k_l \bar{a} H C_{li}}{U_g \varepsilon_g C_{gi}}$ [-]
μ_l : Viscosity of the liquid phase [-]
μ_m : Maximum growth rate [sec^{-1}]
ρ : Density [g/cm^3]
σ : Surface tension [g/cm]
Φ : $3.012(r_{bd}\kappa_o)^{0.55} D_{ec}^{0.45} r_P^{-0.9}$
χ : Biomass concentration [g/cm^3]
ω : $\Phi \frac{\varepsilon_s H}{U_l \varepsilon_l} C_{li}^{-0.35}$ [-]

Subscripts

bd : Dry biofilm
bw : Wet biofilm
g : Gas phase
i : Inlet value
l : Liquid phase
lg : Liquid and gas phase
m : Media
p : Particle
s : Solid phase
T : Total bed

REFERENCES

[1] Schügerl, K. (1997) Three-phase-biofluidization - Application of three-phase fluidization in the biotechnology - A review. *Chem. Eng. Sci.* 52: 3661-3668.
[2] Miura, H. and Y. Kawase (1997) Hydrodynamics and mass transfer in three-phase fluidized beds with non-Newtonian fluids. *Chem. Eng. Sci.* 52: 4095-4104.
[3] Chatib, B., A. Grasmick, S. Elmaleh and R. B. Aim (1981), Biological wastewater treatment in a three-phase fluidised-bed reactor. p. 192-204 In: P. F. Cooper and B. Atkinson (eds.), *Biological Fluidized Bed Treatment of Water and Wastewater.* Ellipse Horwood Limited, Chichester, UK.
[4] Sutton, P. M., J. Hurvid, and M. Hoeksema (1999) Biological fluidized-bed treatment of wastewater from byproduct coking operations: Full-scale case history. *Water Environ. Fed.* 71: 5-9.
[5] Chang, H. T., B. E. Rittmann, D. Amar, R. Hein, O. Ehlinger, and Y. Lesty (1991) Biofilm detachment mechanisms in a liquid-fluidized bed. *Biotechnol. Bioeng.* 38: 499-505.
[6] Choi, J. W. (1983) A theoretical study of the oxygen reaction rate in a three-phase fluidized bed biofilm reactor, M. S. Thesis, Sogang University, Korea.
[7] Mulcahy, L. T., W. K. Shieh, and E. J. Lamotta (1980) Simplified mathematical models for a fluidized bed biofilm reactor. *AIChE Symp. Ser.; Water*: 273-285.
[8] Shieh, W. K., P. M. Sutton, and P. Kos (1981) Predicting reactor biomass concentration in a fluidized-bed system. *J. Water Pollut. Control Fed.* 53: 1574-1584.
[9] Shieh, W. K., A. M. Asce, and L. T. Mulcahy (1981) Fluidized bed for biological wastewater treatment. *J. Environ. Eng. Division.* EE1: 293-295.
[10] Bailey, J. E. and D. F. Ollis (1986) *Biochemical Engineering Fundamentals,* 2nd ed. McGraw-Hill Book Co. New York, NY.
[11] Shieh, W. K. (1980) Suggested kinetic model for the fluidized-bed biofilm reactor. *Biotechnol. Bioeng.* 22: 667-676.
[12] Andrews, G. (1988) Effectiveness factors for bioparticles with monod kinetics. *Chem. Eng. J.*, 37: B31-B37s.
[13] ϕ stergaad, K. and P. Fosbol (1979) Transfer of oxygen across the gas-liquid interface in gas-liquid fluidised beds. *Chem. Eng. J.* 3: 105- 111.
[14] Dakshinamurty, P., V. Subrahmanyam, and J. N. Rao (1971) Bed porosities in gas-liquid fluidization. *I. & E. C. Des. Develop.* 10: 322-328.
[15] ϕ stergaad, K. (1968), Gas-liquid-particle operations in chemical reaction engineering. p. 71-137 *In*: T. B. Drew, G. R. Cokelet, J. W. Hoopes. Jr and T. Vermeulen (ed.) *Adv. Chem. Eng.* Vol. 7,

Academic Press Inc., New York, NY.
[16] Pavlica, R. T. and J. H. Olson (1970) Unified design method for continuous-contact mass transfer operations. *I. & E. C.*, 62: 45-58.
[17] Shah, Y. T. (1979) *Gas-Liquid-Solid Reactor Design*, McGraw Hill Book Co. New York. NY.
[18] Wehner, J. F. and R. H. Wilhelm (1956) Boundary conditions of flow reactor. *Chem. Eng. Sci.* 6: 89-93.
[19] El-Temtany, S. A., Y. O. El-Sharnoubi, and M. M. El-Halwagi (1979) Liquid dispersion in gas-liquid fluidized Beds. *Chem. Eng. J.* 18: 151-159.
[20] Fan, L. S. (1989) *Gas-Liquid-Solid Fluidization Engineering*, Butterworths, Boston, MA.
[21] Williamson, K. and P. l. McCarty (1976) A model of substrate utilization by bacterial films. *J. Water Pollut. Control Fed.* 48: 281-296.
[22] Maron, M. J. (1982) *Numerical Analysis; A Practical Approach*, Macmillan, New York, NY.
[23] Metzler, C. M., G. L. Elfring and A. J. McEwen (1974) A package of computer programs for pharmacokinetic modeling. *Biometrics*, 30: 562-563.